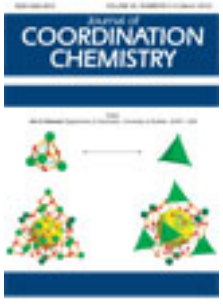

Journal of Coordination Chemistry
Publication details, including instructions for authors and subscription information:
http://www.tandfonline.com/loi/gcoo20

Isolation and spectral studies of water-soluble η^5-cyclichydrocarbon rhodium and iridium complexes with pyridyl diketone analogues bonded through κ^2-NՈO, κ^4-NՈO, and κ^3 -N-C-N modes

Saphidabha L. Nongbri [a] , Babulal Das [b] & Kollipara Mohan Rao [a]
[a] Department of Chemistry , North Eastern Hill University , Shillong 793 022 , Meghalaya , India
[b] Department of Chemistry , Indian Institute of Technology , Guwahati , Assam , India
Published online: 24 Feb 2012.

Journal of Coordination Chemistry
Vol. 65, No. 5, 10 March 2012, 875–890

Isolation and spectral studies of water-soluble η^5-cyclichydrocarbon rhodium and iridium complexes with pyridyl diketone analogues bonded through κ^2-N∩O, κ^4–N∩O, and κ^3-N-C-N modes

SAPHIDABHA L. NONGBRI†, BABULAL DAS‡ and KOLLIPARA MOHAN RAO*†

†Department of Chemistry, North Eastern Hill University, Shillong 793 022, Meghalaya, India
‡Department of Chemistry, Indian Institute of Technology, Guwahati, Assam, India

(*Received 21 September 2011; in final form 2 January 2012*)

The reaction of $[Cp^*M(\mu\text{-}Cl)Cl]_2$ (M = Rh, Ir; $Cp^* = \eta^5\text{-}C_5Me_5$) with 1-phenyl-3-(2-pyridyl) propane-1,3-dione (*pppdH*) and 1,3-di(2-pyridyl)propane-1,3-dione (*dppdH*) in 1 : 2 and 1 : 1 molar ratio, respectively, yielded corresponding monomeric complexes $[Cp^*M(\kappa^2\text{-N-O-}pppdH)Cl]^+$ [M = Rh (**1**), Ir (**2**)] and dimeric complexes $[(Cp^*)_2M_2(\kappa^4\text{-N-O-}dppd)Cl_2]^+$ [M = Rh (**3**), Ir (**4**)]. The treatment of $[Cp^*Ir(\mu\text{-}Cl)Cl]_2$ with *dppdH* in 1 : 2 molar ratio yielded the activated monomeric complex $[Cp^*Ir(\kappa^3\text{-N-C-N-}dppd)]^+$ (**5**). The formation of a $C(sp^3)$–H is attributed to softer iridium, whereas Cp^*Rh precursor yielded only the corresponding dimer **3**. The formation of these complexes has been established by IR and NMR spectroscopic data and elemental analysis. Molecular structures of **2**, **3**, and **5** have been confirmed by single-crystal X-ray diffraction. The enolic "*O–C–C–C–O*" fragment of the coordinated ligand is neutral (κ^2-N-O-*pppdH*) in monomeric **1** and **2** and neutral as well as concomitantly uninegative (κ^4-N-O-*dppd*) in dimeric **3** and **4**. In C–H-activated monomeric complex **5**, the "*O–C–C–C–O*" fragment is in ketonic form with (κ^3-N-C-N-*dppd*) bonding of the ligand.

Keywords: 1-Phenyl-3-(2-pyridyl)propane-1,3-dione; 1,3-Di(2-pyridyl)propane-1,3-dione; Rhodium; Iridium; Pentamethylcyclopentadienyl; C–H activation

1. Introduction

Interest in half-sandwich pentamethylcyclopentadienyl (Cp*) rhodium and iridium complexes started with the development of convenient synthetic methods by Kang and Maitlis [1]. The chemistry of Cp* complexes of rhodium and iridium have been reviewed [2]; these complexes [3, 4] have significant catalytic and synthetic activity in the development of new organometallic compounds. Organometallic complexes of η^5-half sandwich complexes of rhodium and iridium are useful in catalytic asymmetric syntheses [5, 6]. In 1979, Rigby *et al*. [7] reported Cp*Rh(III) complexes of monoanionic

*Corresponding author. Email: mohanrao59@gmail.com

ISSN 0095-8972 print/ISSN 1029-0389 online © 2012 Taylor & Francis
http://dx.doi.org/10.1080/00958972.2012.664638

bidentate *O*,*O*′-ligands. Series of half-sandwich η^5-pentamethylcyclopentadienyl rhodium and iridium complexes possessing *N*, *N*-ligands were also reported [8, 9]. The chemistry of such complexes was broadened where some were used as starting precursors for an extensive synthesis of multinuclear structural designs [10, 11], as catalysts [12, 13], for biological research [14, 15], and in particular water-soluble complexes have attracted considerable interest as potential anticancer, antitumor, and antibacterial agents [16–20]. However, complexes of rhodium- and iridium-containing mixed functional ligands (N∩O) have evolved only recently with the introduction of chelating carboxylate pyrazine ligands [21] and quinolin-8-olate [22]. The η^5-half sandwich water-soluble metal complexes with N∩O ligands were reported to demonstrate anti-tumor and anti-cancer activities [16, 22] and have also been exploited in biological studies [23].

Recently, we reported η^6-arene ruthenium complexes of pyridyl functionalized β-diketones [24]; the chemistry in the previous report encouraged us to synthesize and study pyridyl functionalized β-diketone derivatives possessing Cp*Rh/Cp*Ir fragments. The β-diketonate core is an electron-rich moiety in which the introduction of a polar group like pyridine could modify the dispersive forces and intermolecular interactions [25]; the mono- and di-pyridyl functionalized β-diketone ligands employed in this study, namely 1-phenyl-3-(2-pyridyl)propane-1,3-dione (*pppdH*) [26] and 1,3-di(2-pyridyl) propane-1,3-dione (*dppdH*) [27] coexist as keto-enol tautomers (scheme 1). Royer *et al.* [28] described the coordination chemistry of the tautomeric pair 2-hydroxypyridine/2-pyridone whereby complexes with *O*-bonded pyridones are common with hard metals, whereas softer metals prefer *N*-bonded. Concerned with η^6-arene ruthenium complexes, we established the hetero donor coordination of the N∩O derivatives in which the electronic delocalization of the β-diketonate core appears to be a favorable factor for the existence of η^6-arene ruthenium complexes in the enolic form [24]. Taking into account the above consideration as well as the presence of mixed functional

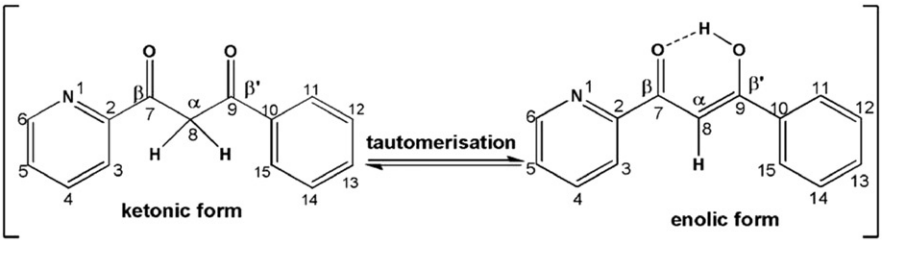

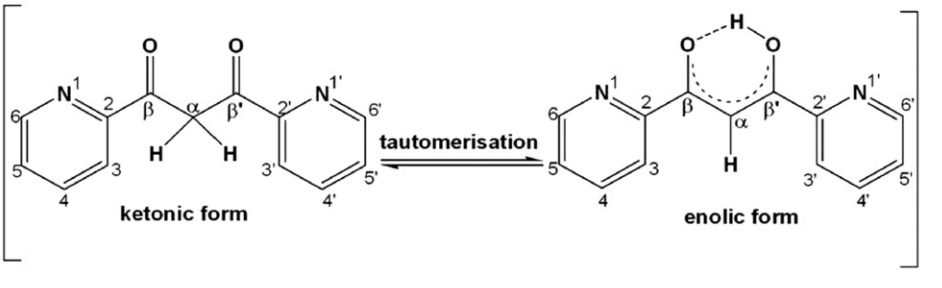

Scheme 1. Ligands used in this study.

donors in the pyridyl functionalized β-diketone, we now synthesize new Cp*Rh/Cp*Ir derivatives of the ligands.

Interest in the synthesis and characterization of metal complexes with mono- and di-pyridyl functionalized β-diketones arises from their potential application in supramolecular chemistry [29, 30] and polynuclear clusters [31, 32]. η^6-Arene ruthenium(II) complexes exist with κ^2-N-O and κ^4-N-O modes of binding of mono- and di-pyridyl functionalized β-diketones [24]; introduction of bulkier electron releasing Cp* and use of rhodium(III) and iridium(III) compared to ruthenium(II) reveal interesting modes of binding of the pyridyl functionalized β-diketone derivatives with the Cp*M(III) fragments (M = Rh, Ir). In this communication we establish the formation of new N∩O-bonded Cp* rhodium and Cp* iridium complexes with κ^2-N∩O, κ^3-N-C-N (C–H activation) and κ^4-N∩O bonding of the ligands.

The unanticipated κ^3-N-C-N mode of binding of *dppd* to Ir(III) occurs through C–H activation of α carbon (sp^3). C–H activation in complexes of Cp*Ir(III) fragments has been extensively studied by Bergman and co-workers [33]. The electron-rich Cp*Ir(III) fragments are potentially useful in C–H activation of alkyl as well as hydrido iridium(III) centers. Primary and secondary amines coordinated to half sandwich complexes of Ru(II)-, Rh(III)-, and Ir(III)-assisted C–H and N–H activation [34]. Self-assembly macrocycles were developed by double site C–H activation of aromatic bis-imine substrates of Cp*Ir(III) complexes [35]. However, there were no previous evidences on the intramolecular C–H activation of pyridyl functionalized β-diketone.

Herein we report the first bis-pyridyl β-diketone intramolecular C–H activated complex of iridium, along with the synthesis of water-soluble complexes having Cp* and 1-phenyl-3-(2-pyridyl)propane-1,3-dione (*pppdH*) or 1,3-di(2-pyridyl)propane-1,3-dione (*dppdH*) as ligands.

2. Experimental

2.1. *Physical measurements*

All reactions were carried out under aerobic conditions using dried solvents. All solvents were dried using appropriate drying reagents and distilled. $RhCl_3 \cdot 3H_2O$ and $IrCl_3 \cdot 3H_2O$ were purchased from Arora Mathey Ltd., and used as received. The precursor $[Cp^*M(\mu\text{-}Cl)Cl]_2$ (M = Rh, Ir; $Cp^* = \eta^5\text{-}C_5Me_5$) [1] and the ligands 1-phenyl-3-(2-pyridyl)propane-1,3-dione (*pppdH*) [26] and 1,3-di(2-pyridyl)propane-1,3-dione (*dppdH*) [27] were prepared using literature protocols. NMR spectra were obtained using a Bruker Avance II 400 spectrometer in acetone-d_6. Chemical shifts were reported as parts per million (ppm, δ), ^1H and ^{13}C chemical shifts are referenced to TMS as an internal standard. Infrared (IR) spectra were recorded as KBr pellets on a Perkin-Elmer 983 spectrophotometer. Elemental analyses were performed in a Perkin-Elmer-2400 CHNS analyzer.

2.2. *Single crystal X-ray structure analyses*

Crystals suitable for X-ray diffraction of **2** and **5** were obtained at room temperature by slow diffusion of hexane over dichloromethane solution of the corresponding complexes. Crystal of **3** was obtained from MeOH solution. Crystals of complexes

Table 1. Crystallographic and structure refinement parameters for **2**, **3**, and **5**.

	2	**3**	**5**
Empirical formula	$C_{25}H_{28}NO_2Cl_3PF_6Ir$	$C_{34}H_{47}N_2O_5Cl_2PF_6Rh_2$	$C_{23}H_{24}N_2O_2PF_6Ir$
Formula weight	818.00	985.43	697.61
Temperature (K)	296(2)	296(2)	296(2)
Wavelength (Å)	0.71073	0.71073	0.71073
Crystal system	Orthorhombic	Monoclinic	Monoclinic
Space group	*P2(1)2(1)2(1)*	*P2(1)/c*	C2/c
Crystal color and shape	Dark red plates	Orange block	Orange block
Unit cell dimensions (Å, °)			
a	8.4116(2)	16.998(2)	24.2090(8)
b	15.3164(4)	15.246(2)	14.5345(6)
c	22.8950(6)	16.434(2)	15.4067(6)
β	90	108.351(8)	119.075(2)
Volume (Å^3), *Z*	2949.69(13), 4	4042.4(9), 4	4737.9(3), 8
Calculated density (Mg m^{-3})	1.842	1.619	1.956
Absorption coefficient (mm^{-1})	4.915	1.057	5.775
F(000)	1592	1992	2704
Crystal size (mm^3)	0.28 × 0.22 × 0.12	0.24 × 0.18 × 0.12	0.30 × 0.18 × 0.10
Scan range (°)	$1.60 < \theta < 27.72$	$1.26 < \theta < 25.00$	$1.70 < \theta < 28.35$
Index ranges	$-10 \le h \le 10$; $-19 \le k \le 19$; $-28 \le l \le 29$	$-20 \le h \le 20$; $-17 \le k \le 17$; $-19 \le l \le 19$	$-32 \le h \le 32$; $-19 \le k \le 19$; $-20 \le l \le 20$
Reflections collected	32,695	40,598	36,812
Independent reflections (R_{int})	6603 (0.0413)	6998 (0.0922)	5871 (0.1306)
Completeness to θ (%)	27.72–97.3	25.00–98.4	28.35–98.9
Absorption correction	Semi-empirical from equivalents	None	None
Refinement method	Full-matrix least-squares on F^2	Full-matrix least-squares on F^2	Full-matrix least-squares on F^2
Data/restraints/parameters	6603/0/358	6998/0/475	5871/0/323
Goodness-of-fit on F^2	0.841	1.048	0.828
Final *R* indices [$I > 2\sigma(I)$][a]	$R_1 = 0.0409$, $wR_2 = 0.1099$	$R_1 = 0.0810$, $wR_2 = 0.1789$	$R_1 = 0.0481$, $wR_2 = 0.1232$
R indices (all data)	$R_1 = 0.0547$, $wR_2 = 0.1200$	$R_1 = 0.1298$, $wR_2 = 0.2293$	$R_1 = 0.0539$, $wR_2 = 0.1278$
Largest difference peak and hole (e Å^{-3})	0.834 and –0.535	0.623 and –0.619	1.205 and –0.927

[a]Structures were refined on F_o^2: $wR_2 = [\Sigma[w(F_o^2 - F_c^2)^2]/\Sigma w(F_o^2)^2]^{1/2}$, where $w^{-1} = [\Sigma(F_o^2) + (aP)^2 + bP]$ and $P = [\max(F_o^2, 0) + 2F_c^2]/3$.

[Cp*Ir(κ^2-N-O-*pppdH*)Cl]$^+$ **2**, [Cp*$_2$Rh$_2$(κ^4-N-O-*dppd*)Cl$_2$]$^+$ **3**, and [Cp*Ir(κ^3-N-C-N-*dppd*)]$^+$ **5** were mounted on a Stoe-Image Plate Diffraction system equipped with a ϕ circle goniometer, using Mo-Kα graphite monochromated radiation ($\lambda = 0.71073$ Å) with a ϕ range of 0–200° in increments of 1.2°, and D_{max}–D_{min} = 12.45–0.81 Å. X-ray intensity data were collected using a Bruker SMART APEX-II CCD diffractometer, equipped with a fine focus 1.75 kW sealed tube Mo-Kα graphite monochromated radiation at 296(2) K, with a 0.3° ω scan mode at a scan speed of 3 s per frame. SMART [36] software was used for data acquisition. Data integration and reduction were undertaken with SAINT [37]. Structures were solved by direct methods using SHELXS-97 [37] and refined with full-matrix least-squares on F^2 using SHELXL-97 [38]. All non-hydrogen atoms were refined anisotropically. Hydrogen atoms were located from difference Fourier maps and refined. Structural illustrations have been drawn with ORTEP-3 [39] for Windows. Data collection parameters are presented in table 1.

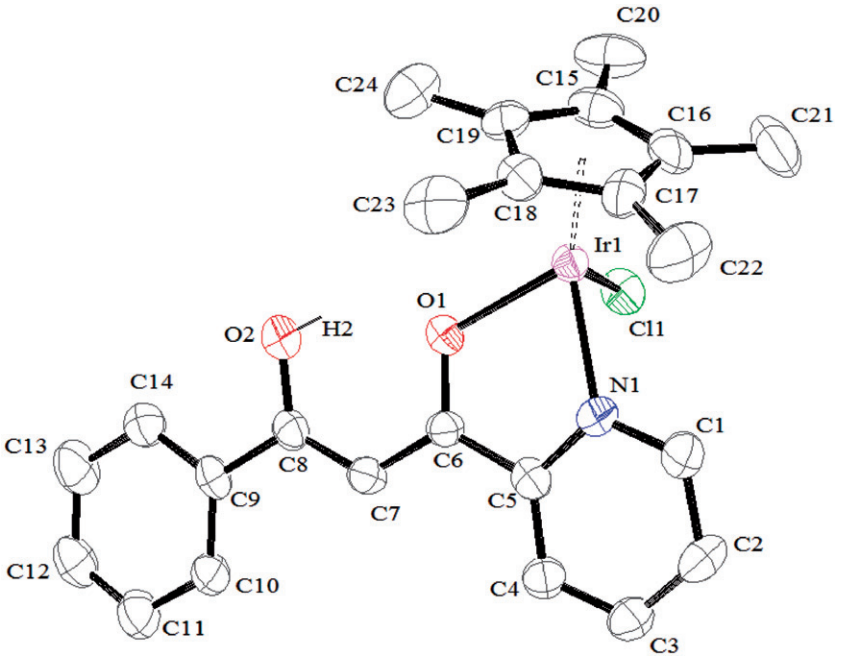

Figure 1. Molecular structure of [Cp*Ir(κ^2-N-O-*pppdH*)Cl]PF_6 **2** with atom numbering scheme. Thermal ellipsoids are depicted with 35% probability level. Hydrogen atoms are omitted for clarity except for the H2 atom. Selected bond lengths (Å) and angles (°): Ir1–cent 1.773, Ir1–O1 2.133(5), C6–O1 1.289(9), C8–O2 1.311(10), C5–C6 1.476(12), C6–C7 1.410(11), C7–C8 1.360(11), C8–C9, 1.471(11), C5–N1 1.346(11), Ir1–N1 2.095(7), O2–H2 0.8200, N1–C5–C6 113.0(7), O1–C6–C5 116.2(7), O1–C6–C7 119.2(7), C6–C7–C8 123.9(8), O2–C8–C7 122.5(7), C5–N1–Ir1 118.1(6), C6–O1–Ir1 117.5(7), O1–Ir1–N1 75.0(2), C8–O2–H2 109.5.

Figures 1–3 are the ORTEP representations of the molecules with 35% probability thermal ellipsoids.

2.3. *Synthesis of 1 and 2*

To a solution of 1 equivalent of *pppdH* (~ 0.06 mmol) in dry methanol, ½ equivalent of the corresponding starting dimer $[Cp^*M(\mu\text{-}Cl)Cl]_2$ (M = Rh, Ir) was added. The resulting solution was stirred and compound started precipitating after ½ h; stirring was continued to complete the reaction. The precipitate was centrifuged and washed with hexane (2 × 2 mL) and diethyl ether. The filtrate was dried by rotary evaporator, the residue was dissolved in dichloromethane (10 mL), and the solution was filtered to remove ammonium chloride and excess ammonium salt. The solution was concentrated to 2 mL, whereupon the addition of excess diethyl ether precipitated the complex which was separated and dried under vacuum as crude product.

2.3.1. [Cp*Rh(κ^2-N-O-*pppdH*)Cl]PF_6 (1). Color: yellow; Yield = 99 mg (78%); IR (KBr, cm^{-1}): 3443 $\nu_{(O-H)}$, 1646 $\nu_{(C=O)}$, 1454 $\nu_{(C-Naromatic)}$, 850 $\nu_{(P-F)}$; Elemental Anal. Calcd for $C_{24}H_{26}NO_2ClPF_6Rh$ (%): C 43.79; H 3.99; N 2.22; Found (%): C 43.81; H

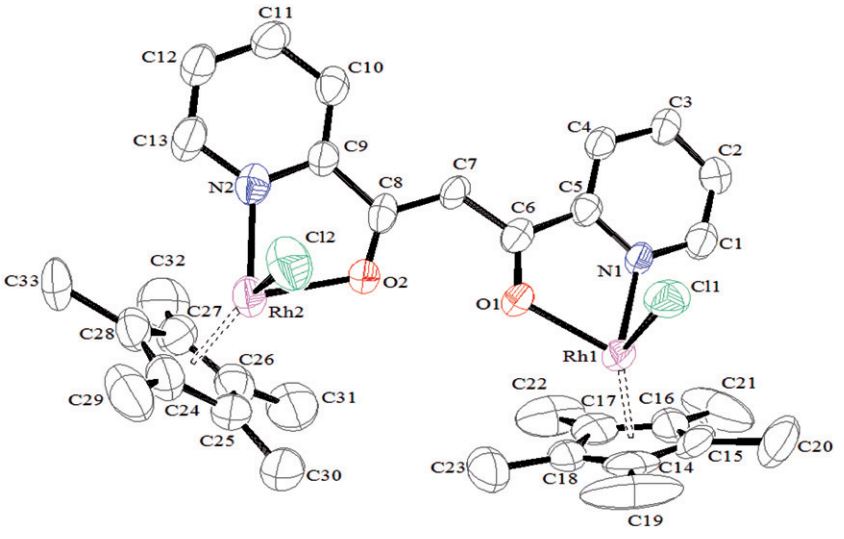

Figure 2. Molecular structure of $[Cp^*_2Rh_2(\kappa^4\text{-N-O-}dppd)Cl_2]PF_6$ **3** with atom numbering scheme. Thermal ellipsoids are depicted with 35% probability level. Hydrogen atoms are omitted for clarity. Selected bond lengths (Å) and angles (°): Rh1–cent 1.765, Rh2–cent 1.759, Rh1–O1 2.097(7), Rh2–O2 2.115(7), C6–O1 1.266(12), C8–O2 1.255(12), C5–C6 1.484(14), C6–C7 1.405(13), C7–C8 1.408(13), C8–C9 1.481(12), Rh1–N1 2.102(8), Rh2–N2 2.121(9), N1–C5–C6 113.2(10), O1–C6–C5 116.4(9), O1–C6–C7 123.4(10), C6–C7–C8 124.9(10), O2–C8–C7 124.8(10), O2–C8–C9 117.5(9), N2–C9–C8 113.1(8), C5–N1–Rh1 115.3(7), C9–N2–Rh2 115.6(6), C6–O1–Rh1 117.8(6), C8–O2–Rh2 117.8(6), O1–Rh1–N1 76.2(3), O2–Rh2–N2 78.8(3).

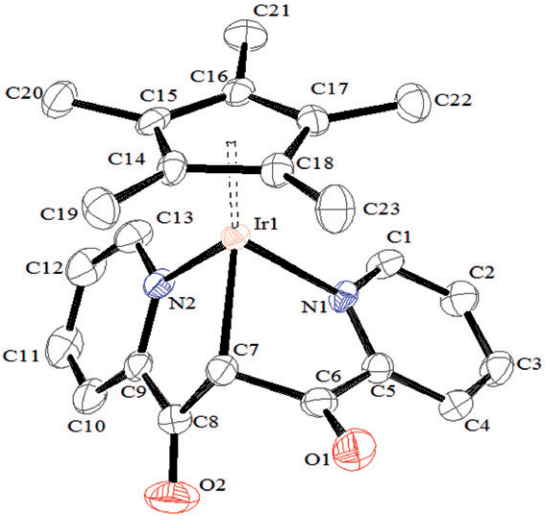

Figure 3. Molecular structure of $[Cp^*Ir(\kappa^3\text{-N-C-N-}dppd)]PF_6$ **5** with atom numbering scheme. Thermal ellipsoids are depicted with 35% probability level. Hydrogen atoms are omitted for clarity. Selected bond lengths (Å) and angles (°): Ir2–cent 1.817, Ir2–N1 2.112(5), Ir2–N2 2.107(5), Ir2–C7 2.099(6), C6–O1 1.206(7), C8–O2 1.203(8), C5–C6 1.510(9), C6–C7 1.490(8), C7–C8 1.592(9), C8–C9 1.479(9), C5–N1 1.351(7), C9–N2 1.347(8), N1–C5–C6 112.9(5), C7–C6–C5 112.4(3), O1–C6–C7 126.6(6), C6–C7–C8 110.0(5), Ir1–C7–C8 109.9(4), C6–C7–Ir1 104.1(4), C9–C8–C7 116.0(5), O2–C8–C7 122.5(7), N2–C9–C8 114.9(5), Ir1–N1–C5 113.7(4), Ir1–N2–C9 117.5(4), N1–Ir1–C7 78.3(2), N1–Ir1–C7 80.9(2), N1–Ir1–N2 86.0(2).

3.97; N 2.25; ^{1}H NMR (acetone-d_6, δ): 1.91 (s, 15 H, C_5Me_5), 7.62 (t, 2 H, H12, H14-pppdH), 7.71 (s, 1 H, α-CH), 7.80 (t, 1 H, H13-pppdH), 8.12 (t, 1 H, H5-pppdH), 8.28 (d, 2 H, $J_{H-H} = 7.6$, H11, H15-pppdH), 8.45 (t, 1 H, H4-pppdH), 8.93 (d, 1 H, $J_{H-H} = 8$, H3-pppdH), 9.27 (d, 1 H, $J_{H-H} = 5.2$, H6-pppdH).

2.3.2. [Cp*Ir(κ^2-N-O-*pppdH*)Cl]PF_6 (2). Color: yellow; Yield = 86.9 mg (87%); IR (KBr, cm^{-1}): 3429 $\nu_{(O-H)}$, 1646 $\nu_{(C=O)}$, 1454 $\nu_{(C-Naromatic)}$, 854 $\nu_{(P-F)}$; Elemental Anal. Calcd for $C_{24}H_{26}NO_2ClPF_6Ir$ (%): C 38.36; H 3.50; N 1.95; Found (%): C 38.66; H 3.31; N 2.05; ^{1}H NMR (acetone-d_6, δ): 1.60 (s, 15 H, C_5Me_5), 7.68 (t, 2 H, H12, H14-pppdH), 7.80 (s, 1 H, α-CH), 7.82 (t, 1 H, H13-pppdH), 8.14 (t, 1 H, H5-pppdH), 8.30 (d, 2 H, $J_{H-H} = 6.8$, H11, H15-pppdH), 8.48 (t, 1 H, H4-pppdH), 9.06 (d, 1 H, $J_{H-H} = 8$, H3-pppdH), 9.32 (d, 1 H, $J_{H-H} = 5.2$, H6-pppdH).

2.4. *Synthesis of 3 and 4*

The starting dimer [Cp*M(μ-Cl)Cl]$_2$ (M = Rh, Ir) taken in 1 : 1 molar ratio with respect to *dppdH* (~0.035 mmol) in the presence of NH_4PF_6 were stirred in dry methanol at room temperature; an orange to red compound began to precipitate and the reaction was continued for 6 h. The isolation after completion of the reaction was by the same method described (section 2.3) for **1** and **2**.

2.4.1. [(Cp*)$_2$Rh$_2$(κ^4-N-O-*dppd*)Cl$_2$]PF_6 (3). Color: yellow; Yield = 59 mg (73%); IR (KBr, cm^{-1}): 1646 $\nu_{(C=O)}$, 1540 $\nu_{(C=O)}$, 1454 $\nu_{(C-N\ aromatic)}$, 844 $\nu_{(P-F)}$; Elemental Anal. Calcd for $C_{33}H_{39}N_2O_2Cl_2PF_6Rh_2$ (%): C 43.21; H 4.29; N 3.05; Found (%): C 43.48; H 4.17; N 3.22; ^{1}H NMR (acetone-d_6, δ): 1.83 (s, 30 H, C_5Me_5), 7.22 (s, 1 H, α-CH), 7.89 (t, 2 H, H5-dppd), 8.24 (t, 2 H, H4-dppd), 8.57 (d, 2 H, $J_{H-H} = 7.6$, H3-dppd), 9.06 (d, 2 H, $J_{H-H} = 5.2$, H6-dppd).

2.4.2. [(Cp*)$_2$Ir$_2$(κ^4-N-O-*dppd*)Cl$_2$]PF_6 (4). Color: dark orange; Yield = 62 mg (75%); IR (KBr, cm^{-1}): 1646 $\nu_{(C=O)}$, 1553 $\nu_{(C=O)}$, 1460 $\nu_{(C-N\ aromatic)}$, 850 $\nu_{(P-F)}$; Elemental Anal. Calcd for $C_{33}H_{39}N_2O_2Cl_2PF_6Ir_2$ (%): C 36.16; H 3.59; N 2.56; Found (%): C 36.56; H 3.72; N 2.77; ^{1}H NMR (acetone-d_6, δ): 1.85 (s, 30 H, C_5Me_5), 7.08 (s, 1 H, α-CH), 7.83 (t, 2 H, H5-dppd), 8.15 (t, 2 H, H4-dppd), 8.42 (d, 2 H, $J_{H-H} = 8$, H3-dppd), 8.92 (d, 2 H, $J_{H-H} = 4.8$, H4-dppd).

2.5. *Synthesis of [Cp*Ir(κ^3-N-C-N-dppd)]PF_6 (5)*

To a round bottom flask containing 25 mL of dry methanol, [Cp*Ir(μ-Cl)Cl]$_2$ (100 mg, 0.13 mmol) and *dppdH* (58 mg, 0.25 mmol) in 1 : 2 molar ratio were added in the presence of NH_4PF_6. The reaction mixture was stirred for 6 h giving yellow precipitate that was centrifuged and the residue washed with hexane (2 × 2 mL), diethyl ether, and dried in vacuum. Color: orange; Yield = 98 mg (73%); Elemental Anal. Calcd for $C_{23}H_{24}N_2O_2PF_6Ir$ (%): C 39.60; H 3.47; N 4.02; Found (%): C 39.69; H 3.45; N 4.24; IR (KBr, cm^{-1}): 1686 $\nu_{(C=O)}$, 1646 $\nu_{(C=O)}$, 1454 $\nu_{(C-N\ aromatic)}$, 850 $\nu_{(P-F)}$; ^{1}H NMR (acetone-d_6, δ): 2.92 (s, 15 H, C_5Me_5), 4.27 (s, 1 H, α-CH), 7.83 (m, 4 H, H4 and H5,

dppd), 8.19 (dt, 2H, $J_{H-H} = 1.2$, H3, dppd), 9.11 (d, 2H, $J_{H-H} = 5.2$, H6, dppd); ^{13}C NMR (acetone-d_6, δ): 9.02 (s, Me (Cp*)), 64.30 (s, α C (dppd)), 89.96 (s, C (Cp*)), 125.09 (s, C3 (dppd)), 132.55 (s, C5 (dppd)), 139.84 (s, C4 (dppd)), 152.80 (s, C6 (dppd)), 155.76 (s, C2 (dppd)), 197.02 (s, β CO (dppd)).

3. Results and discussion

3.1. *Synthetic aspects*

Similar to arene ruthenium analogues [24], the synthetic strategy required NH_4PF_6 rather than employment of a base for the deprotonation of hydroxyl proton of the ligands; consequently, these complexes are isolated as their PF_6 salt. All complexes were characterized by IR and NMR spectroscopic data, elemental analysis, and UV-visible spectroscopy. Molecular structures of three representative complexes (derived from X-ray crystal data) are presented as well.

3.2. *Monomeric complexes 1 and 2*

$[Cp^*M(\mu\text{-}Cl)Cl]_2$ (M = Rh, Ir) undergo bridge cleavage reaction in 1 : 2 molar ratio with *pppdH* in methanol in the presence of NH_4PF_6 to yield mononuclear complexes $[Cp^*M(\kappa^2\text{-N-O-}pppdH)Cl]^+$ [M = Rh (**1**), Ir (**2**)] (scheme 2). In these reactions, **1** and **2** precipitate as their hexafluorophosphate salts during the reaction. Compounds **1** and **2** are isolated as yellow air stable solids in 78–87% yield. They are insoluble in non-polar solvents, but highly soluble in chlorinated solvents, acetone, and water.

In IR spectra of **1** and **2** $\nu_{C=O}$ is observed at 1646 cm^{-1}, similar to free ligand at 1645 cm^{-1}, making it difficult to conclude that coordination occurs through the *O*,*O*′ donor sites of the β-diketone moiety. However, the IR spectra also show medium intensity bands at 3443–3429 cm^{-1} attributed to $\nu_{(O-H)}$ of *pppdH*, arising from H-bonding of uncoordinated OH in *pppdH* of **1** and **2**. The strong absorption at 850 cm^{-1} corresponding to $\nu_{(P-F)}$ confirmed the ionic nature of the complexes. The existence of free OH band and the ionic character of the complexes clearly indicates the coordination of *pppdH* as a neutral (*N*, *O*) donor rather than the mono-anionic (*O*, *O*′) donor which would have yielded analogous neutral complexes.

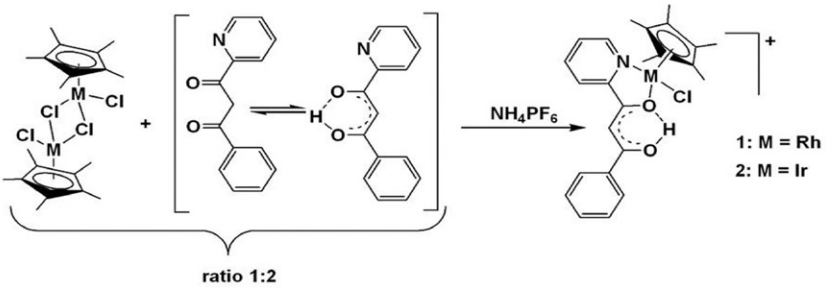

Scheme 2. Preparation of Cp*Rh (**1**) and Cp*Ir (**2**).

To further reveal the coordination behavior of *pppdH*, ^{1}H NMR spectra of **1** and **2** in acetone-d_6 at room temperature are recorded. The Cp* in ^{1}H NMR spectra of **1** and **2** exhibit singlets at δ 1.91 and δ 1.60, respectively, attributable to 15 ring protons. The spectra also display peaks with chemical shifts and multiplicities of three doublets, δ 8.28–8.30 for H11 and H15, δ 8.93–9.06 for H3, and δ 9.27–9.32 for H6 (number scheme in scheme 1) and four triplets, δ 7.62–7.68 for H12 and H14, δ 7.80–7.82 for H13, δ 8.12–8.14 for H5, and δ 8.45–8.48 for H4 (number scheme in scheme 1). The α proton for **1** and **2** is a singlet at δ 7.71 and δ 7.80 correspondingly downfield, indicating the acidic nature of this proton, confirming enolic isomer in solution. However, at room temperature, ^{1}H NMR spectra of **1** and **2** do not show a signal attributable to OH. Inter or intra-molecular hydrogen bonds O–H···O like N–H···N can result in downfield shift of the *pppd*-OH in comparison with the free ligand [40]. Previous publications suggested the occurrence of a broad signal for OH downfield when recorded at very low temperatures [41].

From spectral and synthetic studies, cationic mononuclear complexes **1** and **2** are formed *via* the coordination of *pppdH* as a bidentate neutral *N*, *O* donor in κ^2-N∩O bonding mode. Formation of dimeric complexes of this system could be possible through deprotonation of the uncoordinated O–H and simultaneous C–H activation of the phenyl carbon C15 (number scheme in scheme 1); unfortunately, in spite of various attempts, we were not successful in isolating the expected activated product. To further confirm the bonding modes and structures of **1** and **2** without ambiguity, the molecular structure of [Cp*Ir(κ^2-N-O-*pppdH*)Cl]$^+$ **2** has been carried out.

3.3. *Dimeric complexes 3 and 4*

The dinuclear Cp* complexes [Cp*M(μ-Cl)Cl]$_2$ (M = Rh, Ir) react with one equivalent of the tetradentate, 1,3-di(2-pyridyl)propane-1,3-dione (*dppdH*) in methanol, stirred at room temperature in the presence of NH_4PF_6 to form dinuclear complexes [(Cp*)$_2$M$_2$(κ^4-N-O-*dppd*)Cl$_2$] [M = Rh (**3**), Ir (**4**)] (scheme 3), isolated as their hexafluorophosphate salts in 73–75% yield. These yellow to orange solids are insoluble in non-polar solvents, but soluble in polar solvents and water.

IR spectra of **3** and **4** show lower frequencies of C = O absorption at 1646 cm^{-1} and 1553–1540 cm^{-1}, respectively, compared to that of the free ligand at 1650 cm^{-1} [27].

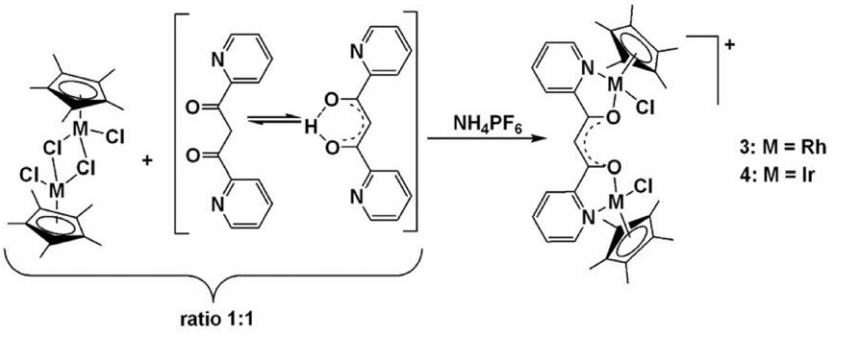

Scheme 3. Preparation of Cp*Rh (**3**) and Cp*Ir (**4**).

However, in addition to hetero donors in the coordinated ligand, resonance probably exists in these complexes, making it difficult to assign the absorption frequency of C=O between the β and β' (number scheme in scheme 1). In contrast to monomeric complexes, no OH absorption band is observed in the IR spectra of **3** and **4**. The ionic nature of these complexes is confirmed by a strong band at 850 cm^{-1} due to the $\nu_{(P-F)}$ of PF_6^-.

To further reveal the coordination of *dppd* to metal, ^{1}H NMR spectra of **3** and **4** in acetone-d_6 were obtained at room temperature. In ^{1}H NMR spectra of **3** and **4**, Cp* exhibits a singlet at δ 1.83 and δ 1.85, respectively, attributable to 30 ring protons of the dimers. The ^{1}H NMR spectra of these complexes support the presence of *dppd* with resonances at δ 7.85–7.89, δ 8.15–8.24, δ 8.42–8.57, and δ 8.92–9.06 as triplet, triplet, doublet, and doublet with multiplicities and chemical shifts comparable to the reported ligand signals [27]. The α proton is observed downfield at δ 7.22 and δ 7.08 for **3** and **4**, respectively, indicating resonance occurring within the β-diketone of the coordinated ligand, resulting in an acidic α proton. A broad low-field resonance ($\delta \sim 15$) characteristic for β-diketone hydrogen-bond for enol tautomers is not observed in the ^{1}H NMR spectra.

Though these complexes are readily soluble in chloroform, the use of acetone-d_6 over $CDCl_3$ in this analysis is advantageous, from the fact that the identification of the acidic α proton is more convenient compared to that in $CDCl_3$ solution where it shows a singlet in the similar region to the acidic α proton.

Similar to arene ruthenium(II) analogues reported earlier, the formation of ionic dimeric complexes is supported by spectral studies of these complexes. Formation of dimeric complexes is possible as the *dppd* ligand is bonded tetradentate in κ^4-N∩O fashion. The serendipitous nature of bonding of the ligand is further confirmed through molecular structures of $[(Cp^*)_2Rh_2(\kappa^4\text{-N-O-}dppd)Cl_2]^+$ (**3**).

3.4. *Monomeric CH activated complex 5*

The reaction of $[Cp^*Ir(\mu\text{-Cl})Cl]_2$ with *dppdH* in 1 : 2 molar ratio, followed by the addition of NH_4PF_6, resulting in the formation of yellow-colored, air-stable monomeric CH-activated complex $[Cp^*Ir(\kappa^3\text{-N-C-N-dppd})]^+$ (**5**) (scheme 4) with solubility similar to **3** and **4**. However, $[Cp^*Rh(\mu\text{-Cl})Cl]_2$ yields only **3** irrespective of precursor complex $[Cp^*Rh(\mu\text{-Cl})Cl]_2$ to ligand (*dppdH*) molar ratio.

Important criteria for controlled and selective carbon hydrogen bond activation are either base-mediated electrophilic addition of organometallic complexes or oxidative addition of low-valent transition metal fragments [42]. In **5**, C–H activation occurs over coordination through *N*, *O* of *dppd* to the metal. Only decomposition of the reaction mixture but no reaction occurs upon treating the dimer $[Cp^*Ir(\mu\text{-Cl})Cl]_2$ with *dppd* in the presence of a base. Consequently, there is no evidence for base-mediated electrophilic addition in the formation of C–H-activated **5**. Formation of C–H activated Ir(III) complexes suggests that the necessary step involves generation of an exceedingly reactive iridium fragment, in formal oxidation state +1, which undergoes an oxidative addition leading to a metal (+3) product containing the new metal carbon bond [43]. $[Cp^*Ir(\mu\text{-Cl})Cl]_2$, upon coordination of ligand *via* mono-anionic *O*, *O'*, would have resulted in chloride cleavage to yield a neutral monomer; the *O*-donor (acac)Ir(III) can activate C–H bonds [44, 45], considering the *O*-donors to be labile due to the

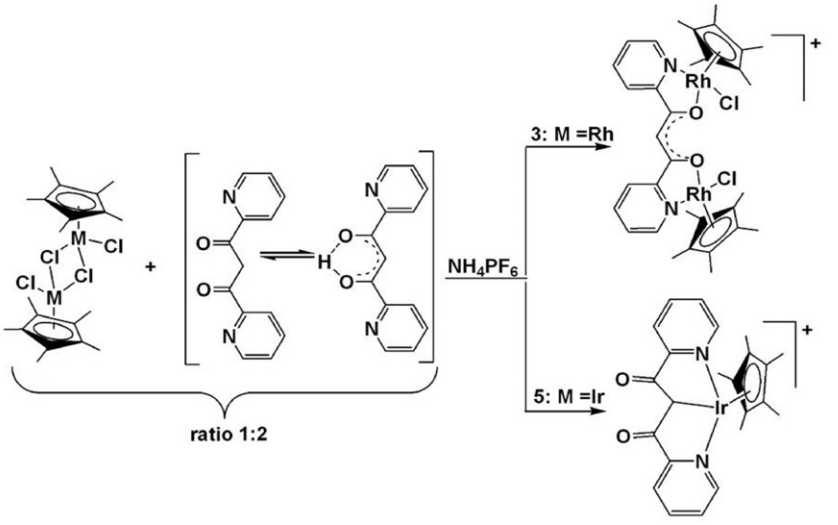

Scheme 4. Comparative presentation on formation of C–H activated $[Cp^*Ir(\kappa^3\text{-N-C-N-}dppd)]^+$ (**5**).

availability of lone pairs of electrons. However, in the present studies, the softer iridium center preferably binds to softer *N*-donor sites [28] of the two pyridyl moieties rather than the *O*-donor sites of the *β*-diketone core of *dppd*, resulting in iridium in +1 oxidation state stabilized by electron-rich Cp*. However, the unstable +1 state rapidly undergoes oxidative addition of *α* carbon with the elimination of hydrogen to yield a negatively charged sp^3 *α* carbon coordinated to iridium with +3 oxidation state. Hence, *dppd* is coordinated as a tridentate donor. Removal of acidic proton is more feasible in the enolic isomer compared to ketonic isomer which is less acidic. Thus, we assume that the ligand may have existed in the enolic form, in an intermediate generated during the reaction. Apart from the mono-anionic Cp* and the negative sp^3 *α* carbon, two half-site occupancy PF_6 counter ions account for a total of one negative charge. Based on previous discussion [46], the coordinated *N*-pyridyl favors C–H activation over *O*-donor sites which have higher electronegativity that could result in the reduction of electron density from the metal center disfavoring oxidative addition [44]. Though density functional theory calculations were not successful on our part, in evaluation of the mechanism involving oxidative addition, we assume formation of the C–H activated complex. Further, spectral analysis reveals anomalous results from **3** and **4** that confirm the formation of C–H activated complex **5**.

The IR spectrum of **5** shows two bands at 1686 and 1646 cm^{-1} for $\nu_{(C=O)}$, characteristic of uncoordinated carbonyl comparable to the free ligand at 1450 cm^{-1} [27]. However, it is not possible to distinguish and assign the relative frequencies for individual carbonyl groups. An intense band at 850 cm^{-1} due to the $\nu_{(P-F)}$ of PF_6^- indicates ionic complex.

The ^1H NMR spectrum of **5** exhibits a singlet at *δ* 2.92 corresponding to 15 protons of Cp*. The ligand exhibits multiplets with chemical shifts and multiplicity varying from those observed for **3** and **4**. A multiplet, a doublet of triplets, and a doublet at *δ* 7.83, 8.19, and 9.11, respectively, for the pyridyl ring protons are observed. The *α* proton resonates at *δ* 4.27 highfield compared to the *α* proton of **3** and **4** which resonates

downfield. This confirms the existence of the α proton in **5** in the ketonic form rather than the enolic isomer observed in **3** and **4**.

The nature of [Cp*Ir(κ^3-N-C-N-*dppd*)]$^+$ **5** is further revealed by ^{13}C NMR studies. The Cp* in **5** displays two singlets at δ 9.02 and 89.96 for methyl carbons and for the ring carbons correspondingly. In addition, *dppd* in this complex displays signals at δ 125.09–155.76 for the pyridyl ring carbons. The α carbon resonates at δ 64.30; in comparison with the ^{13}C NMR spectra of the free ligand, the δ value lies between the value for ketonic and enolic isomers. However, the X-ray structure of this complex confirms the ketonic nature of the ligand when coordinated to Cp*Ir(III), with ligand coordinated in κ^3-N-C-N- fashion to iridium(III). The carbonyl carbons of the diketone exhibit downfield shift of C=O at δ 197.02.

It is not possible to determine the coordination of the ligand from chemical shift data alone. To provide confirming data, X-ray structure analysis is conducted.

3.5. *Molecular structure*

The molecular structures of **2**, **3**, and **5** have been established by single-crystal X-ray structure analysis. X-ray data collection parameters are presented in table 1. Complex **2** is orthorhombic with *P2(1)2(1)2(1)* space group, whereas **3** and **5** are monoclinic with *P2(1)/c* and C2/c space groups, respectively, with only one isomer in the unit cell. The ORTEP structure of **2**, **3**, and **5** are shown in figures 1–3, respectively, along with the selected bond lengths and angles.

The molecular structure of **2** consists of hexafluorophosphate and cation formed by an iridium coordinated to Cp*, to chloride, and to the two hetero atoms of the chelating bidentate *pppdH* forming a three legged ''piano stool'' structure around iridium. One dichloromethane is also present in the crystal. The distance between iridium and the centroid of Cp* of **2** is 1.773 Å. The Ir–O1 and Ir–N1 bond lengths are 2.133(5) Å and 2.095(7) Å, respectively. The bond lengths of the β-diketone core; O1–C6, C6–C7, C7–C8, and C8–O2 (number scheme in figure 1) are 1.289(9) Å, 1.410(11) Å, 1.360(11) Å, and 1.311(10) Å, respectively. The C–O distance of the coordinated carbonyl is 1.289(9) Å and that of the uncoordinated carbonyl is 1.311(10) Å. The bond distances for C5–C6 [1.476(12) Å], C6–C7 [1.410(11) Å], and C7–C8 [1.360(11) Å] are similar, indicating the delocalization of π electrons occurring in the solid state of the complexes. Intramolecular O–H$\cdots$O bonding exists between free OH and coordinated C=O. Although probably fast resonance occurs in the complex, the uncoordinated carbonyl (C8–O2) which is protonated, along with H-bonding, confirms that C7–C8 has double bond character. PF_6^- displays a distorted octahedral geometry. As predicted through the ^{1}H NMR spectrum, the α proton shows acidic nature in solution accounted by the enolic isomer of the ''*O–C–C–C–O*'' fragment; similarly, in spite of delocalization, molecular structure determination confirmed that only the enolic isomer is isolated in the solid state as well.

In **2**, the +3 oxidation state of iridium balanced by mono-anionic Cp*, one chloride, and one PF_6^- indicates that *pppdH* is a neutral bidentate (*N*, *O*) donor, similar to [(η^6-*p*-^{i}PrC$_6$H$_4$Me)Ru(κ^2-N-O-*pppdH*)Cl] [24] where the coordinated *pppdH* ligand is a neutral (*N*, *O*) donor in the enolic form.

In the molecular structure of **3**, each rhodium shows a typical piano-stool geometry with the metal centre coordinated by Cp*, a terminal chloride and a chelating *N*,*O*-

ligand. One molecule of CH_3OH and two molecules of H_2O are present as solvents of crystallization where the hydrogen atoms of the water molecule could not be located. The average distance between Rh to the center of Cp* is 1.76 Å, similar to previous results [8, 9]. The two chlorides of the dimer are *cis* with Rh–Cl average distance of 2.404 Å. The Rh–O and Rh–N distances for both Rh centers are about 2.1 Å. Bond lengths around C5–C6, O1–C6, C6–C7, C7–C8, C8–O2 (figure 2) of the diketone fragment are 1.484(14) Å, 1.266(12) Å, 1.405(13) Å, 1.408(13) Å, and 1.255(12) Å, respectively, for similar reasons as in **2**. Delocalization of π electrons results in similar bond lengths between C6–C7 and C7–C8, which are shorter than adjacent C5–C6 bonds. Consequently, for **3** also only the enolic isomer is isolated, which correlates to the observation of a peak of the α proton in the ^{1}H NMR spectrum of the complex.

In **3** each rhodium center has +3 oxidation state. The charge of the metal center is stabilized by two monoanionic Cp* ligands, two chlorides, and one negative charge from coordinated *dppd*, so the complex has +1 charge which is balanced by hexafluorophosphate. Thus the bridging *dppd* is coordinated as neutral N∩O to one rhodium and $(N\cap O)^-$ to the other rhodium requiring one counter ion (PF_6). Due to delocalization, the C6–O1 and C8–O2 bond lengths are almost the same in **3** and do not distinguish the carbonyl groups, but the formation of mono cationic complexes instead of di-cationic complexes indicate dual nature of *dppd*. The negatively charged *dppd* is delocalized across the "*O–C–C–C–O*" moiety. Rh1–O1 = 2.097(7) Å, Rh2–O2 = 2.115(7) Å, O1–C6 = 1.266(12) Å, O2–C8 = 1.255(12) Å, C6–C7 = 1.405(13) Å, C8–C7 = 1.408(13) Å. The O–C and C–C distances fall midway between single and double bond lengths, as appropriate for delocalized bonding in coordinated *dppd*. Therefore, both coordinating oxygen atoms carry significant and approximately equal, partial negative charge. This behavior of *dppd* was previously observed in $[(\eta^6\text{-arene})_2Ru_2(\kappa^4\text{-N-O-}dppd)Cl_2]^+$ (arene = *p*-^{i}PrC$_6$H$_4$Me, C$_6$Me$_6$). The PF_6^- displays a distorted octahedral geometry in **3**.

Molecular structure determination of **5** reveals a monomeric sp^3 C–H activated κ^3-N-C-N coordination mode of *dppd* (figure 3). The molecular structure of **5** consists of hexafluorophosphate and cation formed by an iridium coordinated to monoionic Cp*, two donor *N*-pyridyl atoms of *dppd*, and sp^3 C–H activated α carbon forming a three legged "piano stool" structure around iridium. In **5**, the ligand is tridentate and facial in contrast to dimeric **3** where the ligand is tetradentate and planar. The distance between the centroid of Cp* and iridium of **5** is 1.817 Å. The Ir–N bond lengths are 2.112(5) Å and 2.107(5) Å, respectively. The bond length between iridium and the activated α carbon is 2.099(6) Å, which is close to the Ir–N bond lengths. The carbonyl of the diketones C6–O1 and C8–O2 have bond distances of 1.206(7) Å and 1.203(8) Å, respectively, while the carbon bond lengths of C6–C7 and C8–C7 of the β-diketonate core ("*O–C–C–C–O*") are 1.490(8) Å and 1.592(9) Å, respectively. C5–C6, C6–C7, C7–C8, and C8–C9 possess single bond character with bond distances of 1.510(9), 1.490(8), 1.592(9), and 1.479(9), respectively. This probably indicates that delocalization of π electrons in the "*O–C–C–C–O*" fragment may not be possible; however, tautomerization of the α proton of the sp^3 C–H-activated moiety may exist. Based on NMR data of this complex, α proton, and α carbon exhibit ketonic isomer in solution, and molecular structure of the complex also confirms isolation of the ketonic form in the solid state as well.

The +3 oxidation state of iridium is balanced by one mono-anionic Cp*, the anionic C–H-activated α carbon and two half-site occupancy PF_6^- counter ions. In contrast to

Table 2. UV-Vis absorption data in acetonitrile at 298 K.

Complex	λ_{max} (nm) ($\varepsilon \times 10^{-4}$ (mol $L^{-1})^{-1}$ cm^{-1})		
1	350 (0.110)	449(0.132)	
2	350 (0.131)		
3	342 (0.161)	443 (0.268)	467 (0.267)
4	350 (0.242)	444 (0.271)	479 (0.249)
5	353 (0.201)	444 (0.220)	476 (0.209)

η^6-arene ruthenium complexes and **3** possessing *dppd*, in **5** the ligand does not coordinate in the κ^4-N∩O fashion through its dual uninegative $(N, O)^-$ and neutral (N, O) donor sites, but is bound through neutral *N*-dipyridyl moiety and the anionic α carbon in κ^3-N-C-N coordination.

From structures in mononuclear **2**, the coordinated *pppdH* is not bonded to iridium in $(O, O')^-$ anionic fashion or $(N, O)^-$ uninegative but as neutral (N, O) donor in enolic form. In dimeric **3** *dppd* exhibits dual nature coordinated to rhodium as neutral (N, O) and uninegative $(N, O)^-$ donors. Coordination of *dppd* in $(O, O')^-$ anionic mode could have accounted for monomeric neutral species. The enolic form is isolated in the solid crystals. Anomalous behavior of *dppd* is also observed in **5**, where the cyclometallation of N∩O does not occur through chelating *O*, *O*′ or *N*, *O*′ but involves the activation of α C(sp^3)–H, resulting in coordination through two neutral *N*-pyridyls. The X-ray analysis of this complex indicated covalent bonding of activated C7–C8, C7–C6, and C7–H7, as well as coordination to the Ir center. This indicates sp^3 hybridization of C7; the C8–C7–C6 angle is 110.28′, representing an sp^3 carbon.

3.6. *UV-visible presentation*

UV-Vis spectra of complexes were acquired in acetonitrile and spectral data are summarized in table 2. Electronic spectra of these complexes are depicted in the "Supplementary material." The energy of these transitions should vary with the nature of the ligand acting as π acceptors [47, 48] and bands on the higher energy side, ~300–400 nm, have been assigned to ligand-centered $\pi \rightarrow \pi^*/n \rightarrow \pi^*$ transitions [49, 50]. The electronic spectra of **1**–**5** display a single band at ~340 nm, attributed to intra ligand π–π^* transition. Monomeric **1** and **2** containing *pppdH* display a lower intense band; however, **3**, **4**, and **5** containing *dppd* have a higher intensity band in the UV region. The electronic spectrum of **2** does not display a band in the visible region, while **1** displays a medium intensity band and **3**, **4**, and **5** show high-intensity bands in the visible region at ~450–480 nm assignable to metal-to-ligand charge-transfer transition (MLCT) (t_{2g}-π^*). The dimeric **3** and **4** and monomeric C(sp^3)–H-activated **5** show a bathochromic shift, more prominent in iridium complexes **4** and **5** with higher intensity bands compared to rhodium complex **3**. These complexes display $\pi \rightarrow \pi^*$ transition for the pyridyl diketone in the UV region and MLCT transition in the visible region as observed in previous reports [8, 9, 21].

4. Conclusion

We report the synthesis of new complexes and confirm their formation through various analyses. Monomeric **1** and **2** are generated by reaction of chloro-bridged dimer with *pppdH* in 1 : 2 molar ratio, 1 : 1 molar ratio yields dimers **3** and **4**, whereas *dppdH* yields C–H-activated **5** when treated with $[Cp^*Ir(\mu\text{-}Cl)Cl]_2$ in 1 : 2 molar ratio. Spectral analyses reveal ionic complexes isolated as their PF_6 salts and **1**, **2**, **3**, and **4** have the enolic isomer in solution and solid state; however, the C–H-activated **5** exists in the ketonic form both in solution and solid state. From molecular structure analysis, *pppdH* coordinates bidentate neutral (*N*, *O*) to the metal center in monomeric complexes in κ^2-*N*∩*O* mode, tetradentate neutral (*N*, *O*), and uninegative (*N*, *O*)$^-$ in dimeric complexes, planar κ^4-*N*∩*O* fashion and tridentate in the C–H-activated complex through two neutral *N*-pyridyl donors and uninegative α carbon in facial κ^3-N-C-N bonding mode.

Supplementary material

CCDC-842580 (**2**), -842581 (**3**), and -842582 (**5**) contain the supplementary crystallographic data for this article. These data can be obtained free of charge *via* www.ccdc.cam.ac.uk/data_request/cif, by e-mailing data_request@ccdc.cam.ac.uk, or by contacting The Cambridge Crystallographic Data Centre, 12 Union Road, Cambridge CB2 1EZ, UK; Fax: +44 1223 336033.

Acknowledgments

S.L. Nongbri thanks UGC-RGNF for financial support in the form of *SRF* bearing fellowship allotment No. *18-16(7)/Acad/2009-77*. K.M. Rao gratefully acknowledges financial support from the CSIR, New Delhi, through the Research grant No. 01(2493)/11/EMR-II.

References

[1] J.W. Kang, P.M. Maitlis. *J. Am. Chem. Soc.*, **90**, 3259 (1968).
[2] P.M. Maitlis. *Acc. Chem. Res.*, **11**, 301 (1978).
[3] G. Wilkinson, F.G.A. Stone, E.W. Abel (Eds). *Comprehensive Organometallic Chemistry II*, Vol. 7, 2nd Edn, Elsevier, Oxford (1995).
[4] F.P. Pruchnik. *Organometallic Chemistry of the Transition Metals*, Plenum, New York (1990).
[5] H. Brunner. *Adv. Organomet. Chem.*, **18**, 151 (1980).
[6] S.G. Davies. *Pure Appl. Chem.*, **66**, 13 (1988).
[7] W. Rigby, H.B. Lee, P.M. Bailey, J.A. McCleverty, P.M. Maitlis. *J. Chem. Soc., Dalton Trans.*, 387 (1979).
[8] K.T. Prasad, G. Gupta, A.K. Chandra, M.P. Pavan, K.M. Rao. *J. Organomet. Chem.*, **695**, 707 (2010).
[9] G. Gupta, K.T. Prasad, B. Das, G.P.A. Yap, K.M. Rao. *J. Organomet. Chem.*, **694**, 2618 (2009).
[10] Y.-F. Han, Y.-J. Lin, L.-H. Weng, H. Berke, G.-X. Jin. *Chem. Commun.*, 350 (2008).
[11] P. Govindaswamy, G. Süss-Fink, B. Therrien. *Inorg. Chem. Commun.*, **10**, 1489 (2007).

[12] F. Hanasaka, K.-I. Fujita, R. Yamaguchi. *Organometallics*, **24**, 3422 (2005).
[13] S.-I. Murahashi, H. Takaya, T. Naota. *Pure Appl. Chem.*, **74**, 19 (2002).
[14] P.J. Dyson, G. Sava. *Dalton Trans.*, 1929 (2006).
[15] M. Auzias, B. Therrien, G. Süss-Fink, P.P. Štěpnička, W.H. Ang, P.J. Dyson. *Inorg. Chem.*, **47**, 578 (2008).
[16] Z. Liu, A. Habtemariam, A.M. Pizarro, S.A. Fletcher, A. Kisova, O. Vrana, L. Salassa, P.C.A. Bruijnincx, G.J. Clarkson, V. Brabec, P.J. Sadler. *J. Med. Chem.*, **54**, 3011 (2011).
[17] M. Gielen, E.R.T. Tiekink (Eds). *Metallotherapeutic Drugs and Metal-Based Diagnostic Agents*, Wiley, Chichester (2005).
[18] A. Dorcier, W.H. Ang, S. Bolano, L. Gonsalvi, L. Juillerat-Jeannerat, G. Laurenczy, M. Peruzzini, A.D. Phillips, F. Zanobini, P.J. Dyson. *Organometallics*, **25**, 4090 (2006).
[19] J. Canivet, G. Suss-Fink, P. Štěpnička. *Eur. J. Inorg. Chem.*, 4736 (2007).
[20] D. Herebian, W.S. Sheldrick. *Dalton Trans.*, 966 (2002).
[21] P. Govindaswamy, B. Therrien, G. Süss-Fink, P. Štěpnička, J. Ludvík. *J. Organomet. Chem.*, **692**, 1661 (2007).
[22] U. Śliwińska, F.P. Pruchnik, S. Ułaszewski, M. Latocha, D. Nawrocka-Musiał. *Polyhedron*, **29**, 1653 (2010).
[23] S. Wirth, C.J. Rohbogner, M. Cieslak, J. Kazmierczak-Baranska, S. Donevski, B. Nawrot, I.-P. Lorenz. *J. Biol. Inorg. Chem.*, **15**, 429 (2010).
[24] S.L. Nongbri, B. Das, K.M. Rao. *J. Chem. Sci.*, MTIC XIV special issue.
[25] M.J. Mayoral, P. Cornago, R.M. Claramunt, M. Cano. *New J. Chem.*, **35**, 1020 (2011).
[26] S.K. Langley, N.F. Chilton, M. Massi, B. Moubaraki, K.J. Berry, K.S. Murray. *Dalton Trans.*, **39**, 7236 (2010).
[27] P.C. Andrews, G.B. Deacon, R. Frank, B.H. Fraser, P.C. Junk, J.G. MacLellan, M. Massi, B. Moubaraki, K.S. Murray, M. Silberstein. *Eur. J. Inorg. Chem.*, 744 (2009).
[28] A.M. Royer, T.B. Rauchfuss, D.L. Gray. *Organometallics*, **28**, 3618 (2009).
[29] Y.-Y. Hui, H.-M. Shu, H.-M. Hu, J. Song, H.-L. Yao, X.-L. Yang, Q.-R. Wu, M.-L. Yang, G.-L. Xue. *Inorg. Chim. Acta*, **363**, 3238 (2010).
[30] S. Brück, M. Hilder, P.C. Junk, U.H. Kynast. *Inorg. Chem. Commun.*, **3**, 666 (2000).
[31] C.-I. Yang, W. Wernsdorfer, Y.-J. Tsai, G. Chung, T.-S. Kuo, G.-H. Lee, M. Shieh, H.-L. Tsai. *Inorg. Chem.*, **47**, 1925 (2008).
[32] J.-P. Tong, F. Shao, J. Tao, R.-B. Huang, L.-S. Zheng. *Inorg. Chem.*, **50**, 2067 (2011).
[33] P.J. Alaimo, B.A. Arndtsen, R.G. Bergman. *Organometallics*, **19**, 2130 (2000).
[34] W.B. Cross, C.G. Daly, Y. Boutadla, K. Singh. *Dalton Trans.*, **40**, 9722 (2011).
[35] H. Li, Y.-F. Han, G.-X. Jin. *J. Organomet. Chem.*, **696**, 2129 (2011).
[36] *XRD: Single-crystal Software*, Bruker Analytical X-ray Systems, Madison, WI, USA (2002).
[37] G.M. Sheldrick. *Acta Cryst.*, **A 46**, 467 (1990).
[38] G.M. Sheldrick. *SHELXL-97*, University of Göttingen, Göttingen, Germany (1999).
[39] L.J. Farrugia. *J. Appl. Cryst.*, **30**, 565 (1997).
[40] G. Albertin, S. Antoniutii, J. Castro, S. Garcia-Fontan. *Eur. J. Inorg. Chem.*, 510 (2011).
[41] N.S. Golubev, S.N. Smirnov, P.M. Tolstoy, S. Sharif, M.D. Toney, G.S. Denisov, H.H. Limbach. *J. Mol. Struct.*, **844**, 319 (2007).
[42] M.R. Crimmin, D.A. Colby, J.A. Ellman, R.G. Bergman. *Dalton Trans.*, **40**, 514 (2011).
[43] K.I. Goldberg, A.S. Goldman (Eds). *Activation and Functionalization of C–H Bonds*, Chap. 2, ACS Symposium Series No. 885, ACS publications, Washington, DC (2004), and references therein.
[44] A.G. Wong-Foy, G. Bhalla, X.Y. Liu, R.A. Periana. *Prepr. Pap.-Am. Chem. Soc., Div. Fuel Chem.*, **48**, 825 (2003).
[45] G. Bhalla, J. Oxgaard, W.A. Goddard III, R.A. Periana. *Organometallics*, **24**, 5499 (2005).
[46] J. Liu, X. Wu, J.A. Iggo, J. Xiao. *Coord. Chem. Rev.*, **252**, 782 (2008).
[47] D.K. Lavallee, M.D. Baughman, M.P. Phillips. *J. Am. Chem. Soc.*, **99**, 718 (1977).
[48] N.G. Del, V. Morena, N.E. Katz, J. Olabe, P.J. Aymonino. *Inorg. Chim. Acta*, **35**, 183 (1979).
[49] P. Didier, I. Ortmans, A.K.D. Mesmacker, R.J. Watts. *Inorg. Chem.*, **32**, 5239 (1993).
[50] B.P. Sullivan, D.J. Salmon, T.J. Meyer. *Inorg. Chem.*, **17**, 3334 (1978).